Automating the 3D robotic filament winding process for high-performance composite materials

Johannes Mersch, Danny Friese, Hung Le Xuan

Automating the 3D robotic filament winding process for high-performance composite materials

*Johannes Mersch** *Danny Friese* *Hung Le Xuan*

Dr.-Ing. J. Mersch, D. Friese, H. Le Xuan
Institute of Textile Machines and High-Performance Materials Technology, Dresden University of Technology, 01062 Dresden, Germany
Email Address: johannes.mersch@tu-dresden.de

Keywords: *robotic filament winding, path planning, automated robot programming, high-performance composite materials, coreless robotic winding*

Robotic filament winding of high-performance materials in 3D geometries presents a promising avenue for advancing lightweight and civil engineering. However, the unique challenges posed by filament winding necessitate the development of novel path planning algorithms. Traditional slicing techniques, commonly used in regular 3D printing, are inadequate due to the complexities of filament winding processes and the utilization of materials with exceptional mechanical properties. In this article, we propose an innovative approach to automate 3D coreless robotic filament winding. The key focus of our work lies in overcoming the limitations of conventional algorithms and addressing the specific boundary conditions associated with diverse applications. Our method builds upon Hierholzer's algorithm that is then expanded to accommodate the intricate constraints of filament winding. We achieve a comprehensive path planning framework capable of navigating complex 3D geometries while optimizing the utilization of high-performance materials. This approach allows efficient and precise filament winding, preserving the ultra-strong mechanical properties of the materials. Furthermore, we demonstrate the conversion of the generated path into a robot program. The outcomes of our research offer promising prospects for various industrial sectors, including aerospace, automotive, and construction industry. This facilitates the utilization of cutting-edge materials in engineering applications in the future.

1 Introduction

Several mega-trends are addressed by the emerging technology of robotic filament winding. On the one hand, it is the need to decrease carbon dioxide emissions. The construction industry currently produces about 37 % of these emissions.[1] Carbon fiber-reinforced concrete, which avoids the corrosion-vulnerability of steel, can drastically decrease the amount of required concrete.[2, 3] On the other hand, with the increasing lack of skilled workers and demographic change, automation, and enhanced productivity become vital, particularly for established economies.[4] Robot-guided winding of high-performance fibers allows to create a highly automated process and simultaneously takes advantage of their extremely anisotropic but excellent mechanical properties. With usual layer-by-layer additive manufacturing processes, for which a plethora of slicing algorithms have been established and commercialized in the last few years, this is not possible. In the last ten years, the use and research of coreless robotic winding (CRW) technologies has been growing both for classic composite applications as well as civil engineering.[5, 6] The winding of reinforcement fibers around core structures is a widely established technology to produce high-performance composites.[7, 8] Using a core is beneficial for some applications, especially for tanks. Because the fibers' superior mechanical properties are only present if they are loaded with tensile stress in fiber direction, the core-wound composites are ideal for pressure vessels or torsionally loaded components such as drive shafts.[9] However, this technology restricts the possibilities of the shape and the fiber orientations on said shape.[10, 11]
A different option to leverage the properties of reinforcement fibers is to disperse short fibers in either concrete or thermoplastic materials, which can then be extruded in layers in an additive process.[12] The options to include reinforcement yarns in layer-by-layer additive manufacturing processes are described by Safari et al..[13] Disadvantages of short fibers and a layer-by-layer process are the lack of adhesion and especially the lack of reinforcement fibers between layers.[14] In addition, the short fiber-reinforced materials have much lower moduli and strength than long fiber-reinforced materials.[15]
Therefore in recent years, coreless robotic winding has been proposed both with polymeric and mineral matrix systems.[16, 17] With the CRW-technology the reinforcement fibers are wound around small winding elements on tubes positioned arbitrarily in space. The winding elements are pin-shaped or have pins

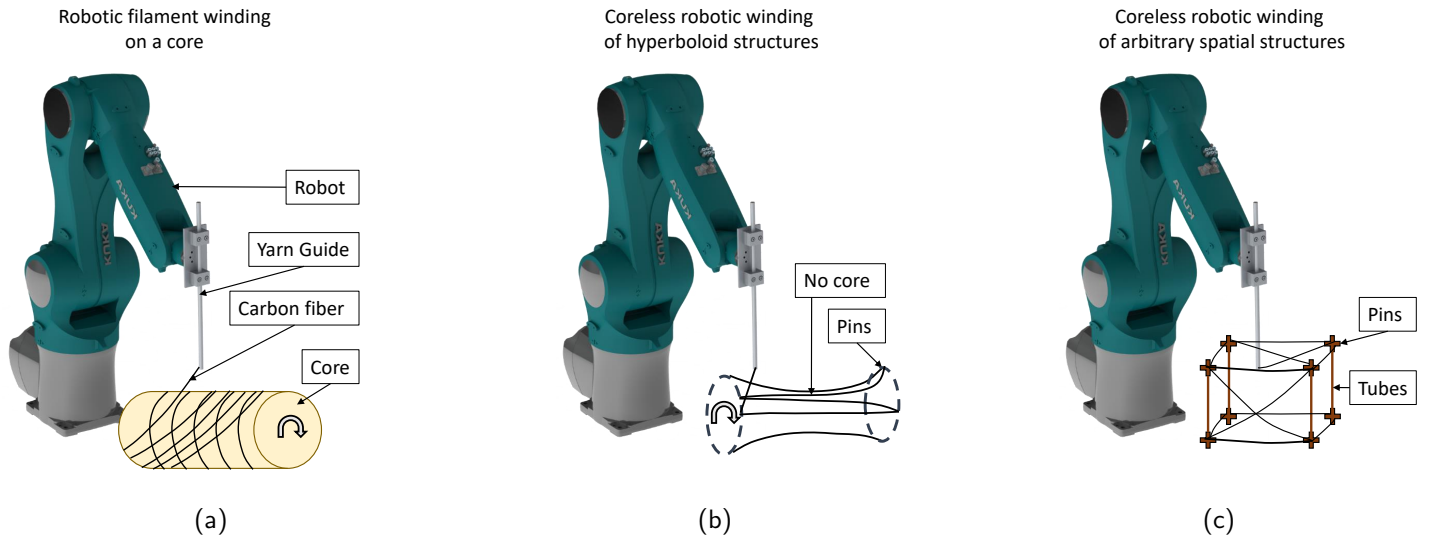

Figure 1: Different types of robotic winding (a) on core (b) coreless hyperboloid according to [16], (c) coreless with crossings and intersections

attached to them that hold the fibers in place. The difference to the classic winding approach is illustrated in **Figure 1c**. Further developments of this approach with complex fiber orientations or fabrics instead of single fibers have been proposed but are still limited to circumferential reinforcements.[18, 19] As demonstrated by Daimler, CRW allows to produce mechanically highly-optimised truss-based composite structures.[20, 21] The growing availability of computational power and efficient algorithms makes the topology optimization for complex load cases feasible within appropriate time frames.[22] The design and topology of such composite truss structures may be derived from a wide variety of approaches.[23] They can range from biologically inspired fiber distributions [24, 25], force-flow approaches [18] to established methods like the solid isotropic material with the penalization (SIMP) interpolation model.[26] Although this is one research area of enormous importance for the further development of composite technology, it is not the focus of this work. How the geometry and truss dimensions are derived from the boundary conditions is not discussed within this work but is taken as a given input to the algorithm. Another essential point that is currently missing on the path to fully automated high-performance composite manufacturing are algorithms for converting the topology optimized truss structure to robotic paths.[27] This poses a challenge, particularly for structures that consist of intersecting and branching fibers in three-dimensional (3D), i.e. out-of-plane reinforcements.[5]

In the last three years two major contributions have been made to the automated path planning for CRW. One is the work of Bodea et al. who focused on hyperboloid structures (see **Figure 1b**), particularly for the construction of pre-assembled building blocks. They used the Grasshopper plug-in for Rhino to create the motion commands for their kinematic system. This leads to large-scale coreless composite structures. Nevertheless, the path planning itself is relatively simple because the component is rotated during the manufacturing process. Therefore, the end-effector is only moving above the surface of the component on quasi-linear curves, which eliminates the risk of collision with the already positioned yarns. At the same time, this approach is limited to hyperboloid shapes. Oval et al. pursued a more general approach for shell structures, in which the winding elements are positioned on curved shells and connected by different amounts of reinforcement fibers.[17] Each winding element can be connected to one or multiple other winding elements. When abstracting the winding elements to nodes and the fibers in between connections, the structure can be represented as a graph. The problem of inserting a certain number of yarns between the nodes represents a version of the chinese postman problem (CSP).[28] One algorithm to solve the CSP is Hierholzer's algorithm and finding Eulerian paths connecting the nodes until all connections have been traveled.[1] After finding a suitable path, Oval et al. derived the robot program by moving around each winding element in circles and between circles by straight lines. This approach is

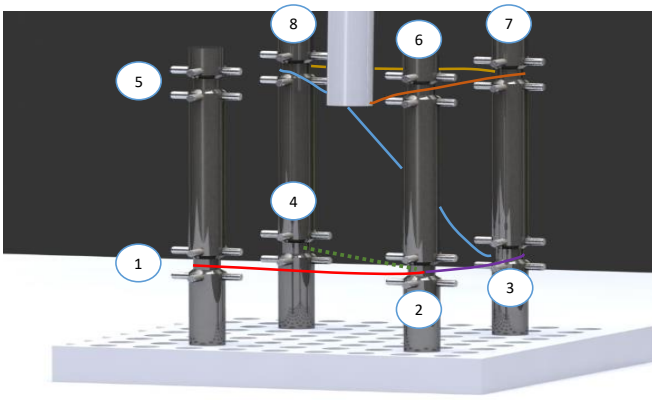

Figure 2: Illustration of a potential collision between the yarn guide and deposited yarns.

sufficient for winding elements distributed on curved surfaces but it cannot deal with connections that are at a larger angle to the x-y-plane or fibers that cross in z-direction as illustrated in Figure 1c. To extend the capabilities of CRW to 3D structures, we propose a new path planning algorithm, which can deal with winding elements, i.e. winding elements, on multiple levels and intersections. The approach is divided into two steps. First, the abstract graph level is considered to leverage the capabilities of established algorithms like the Hierholzer algorithm. Nevertheless, the restrictions of the 3D-CRW technology, where already deposited yarns are obstacles, and other manufacturing-related particularities are considered in our approach. Based on this graph representation, the actual path of the robot's end-effector is derived. Finally, the path for an exemplary structure will be automatically planned and implemented on a small-scale 6-axis robot.

2 Route planning based on graph representation

The input to the algorithm is the positions of the winding elements, which are then considered as nodes in the representation as a graph. These are stored as a list with each node having a number and their position in x, y, and z. Each node is connected to at least one other node by a connection. The connections are usually represented by an adjacency matrix Adj_{orig} where connections or missing connections are ones or zeros, respectively. Here we additionally modify the adjacency matrix, so it contains the numbers of yarns that need to be deposited between two nodes, which is stored as Adj_{ext}. The number of yarns is derived from the desired cross-section area according to the topology optimization and the reinforcement yarn to be used. The Adj_{orig} is still saved to navigate through the graph if the yarns of some connections have already been deposited sufficiently, similar to the rural postman problem.[29] The output of this part of the path planning routine is the ordered sequence of nodes to be connected.

2.1 Restrictions due to collisions

In contrast to the geometry considered by Oval et al., where every winding element can be connected to any other winding element at all times, with multi-level structures and intersections in z-direction, already deposited yarns may block other connections between nodes.[17] This is also a major difference from classic slicing algorithms for other additive manufacturing methods. Consequently, there are three kinds of collisions with the yarn guide, which have to be avoided. First, the yarn guide should not crash into winding elements. Second, the yarn guide should not collide with already deposited yarns while traveling around a winding element. Both of these are dealt with in the spatial path planning. However, the third type of possible collision cannot be avoided in the spatial path planning but has to be addressed during the first step, because if the nodes are not in a feasible order, the winding becomes practically impossible. This is illustrated in **Figure 2**. After winding the connections from nodes 1 - 2 - 3 - 8 - 7, the connection between 2 and 4 (dotted green line) is covered. Therefore, guiding the yarn around node

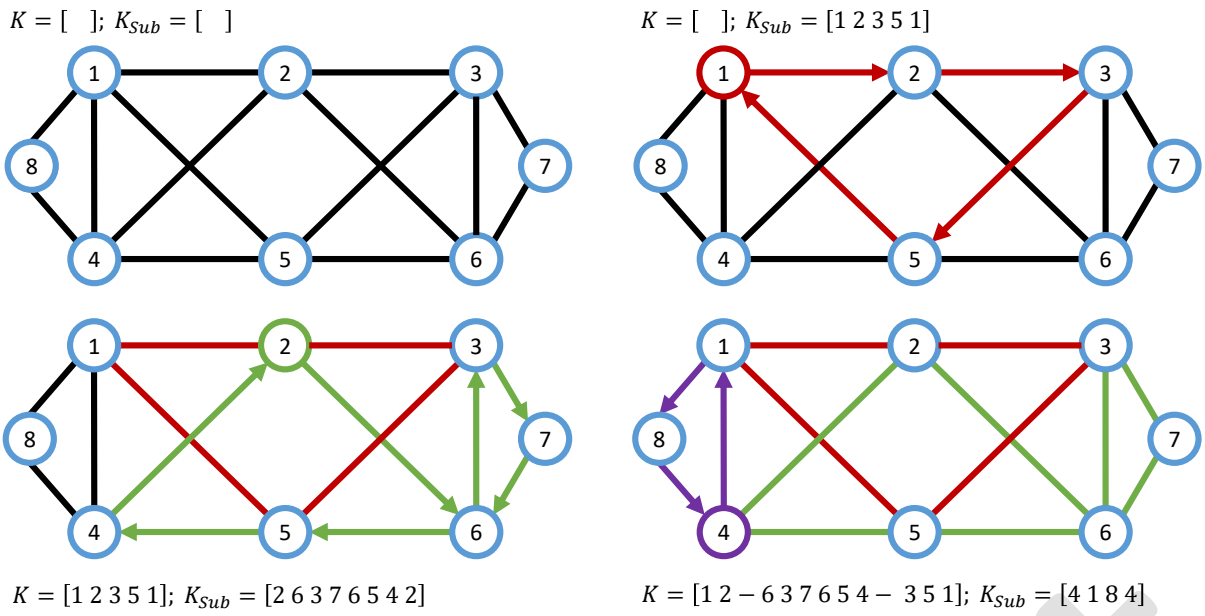

Figure 3: Illustration of the Hierholzer algorithm.

4 would result in a collision with the already deposited yarn between nodes 7 and 8. Such restrictions have to be considered when deriving the node sequence based on the Hierholzer algorithm.

2.2 Hierholzer-based Algorithm

The basic algorithm of Hierholzer is shown in 3 and illustrated in **Figure 3**. The starting node is selected by user input because in practice a dummy node is introduced where the reinforcement yarn is fixed.

Algorithm 1 Basic Hierholzer Algorithm.

while node with open connections exists **do**
  find node with open connections
  find subcircle K_{Sub}
  insert K_{Sub} in overall circle K
end while
return K

As described in the previous subsection, the basic Hierholzer algorithm needs to be expanded to cope with the mentioned restrictions. Therefore, before initializing the algorithm, a check is conducted, which connections cover which connections. The connections covering other connections are then set to zero in the adjacency matrix $Adj_{current}$ until the desired yarn count is reached for the covered connection. In addition, before the subcircle K_{Sub} is inserted, a check is performed, whether K_{Sub} is covered by any connections before the insertion position or covers any connections after the insertion position. If no feasible insertion position is found, K_{Sub} is added to the end of the sequence. The path from the last node of the existing K and the first node of K_{Sub} is calculated using Dijkstra's algorithm based on the Euclidean distances between nodes.[30]

2.3 Process-related improvements of the path planning procedure

In addition, other process- or application-related particularities can be considered and implemented in the algorithm. These mainly concern the specific requirements of fiber-reinforced plastics versus fiber-

reinforced concrete. For example, in many plastic composite applications the matrix material is applied during the winding process or pre-impregnated yarns are used. The structure is then used - as is - after curing. The winding elements can or often should remain in the structure. They either serve as stabilization or are used to join the composite with other parts. It is also possible to use other functional parts such as bearings or sensors as winding elements. Because these winding elements should remain as part of the structure, the adhesion between reinforcement yarn and winding elements is important. Therefore, fully or partially wrapping the yarn around their circumference may be beneficial. In addition, crosses of yarns without a winding element (e.g. the connections 1-5 and 2-4 in Figure 3) should be wound alternately to improve the adhesion and thereby increase shear stability.
For concrete composites, however, the winding elements should be removed, so the concrete can fill their space, to fix the reinforcement structure and to avoid porous areas which are potential crack initiation points. In such applications, long sections of yarns without deviations of large angles are preferred to maximise the load-bearing capacity of the reinforcement yarns. Moreover, we found that disfavoring connections that go from lower to higher positioned nodes helps to avoid the blocking of yarns, and thus, makes the algorithm faster for the configurations we tested. Without this feature, dead ends occur regularly. Because other than in a normal Eulerian path:

- Connections can require multiple visits by the postman (i.e. yarn depositions),
- number of visits can vary drastically between connections based on the topology optimization and
- nodes can have an uneven number of connections.

Therefore, nodes without feasible connections can be encountered during the construction of K_{Sub}. In that case, the current K_{Sub} is stored and a new subcircle is initiated at another node. If no successful subcircle can be constructed starting from one of the nodes with remaining connections, a sub-routine is initiated. This is a classic genetic algorithm with the order of nodes to be connected as the genome. The result is a close-to-optimal path between nodes of the missing yarns that don't cover other connections, which are connected via feasible connections according to $Adj_{current}$. That is necessary because not all or realistically very few application-relevant structures can be wound as perfect Eulerian circles or paths. Thereby, the amount of excess deposited material and consequently weight is minimized. Apart from the savings in the amount of material, any winding of excess yarns increases the overall process length. Therefore, procedures that keep the yarn number and distribution as close as possible to the result of the topology optimization are advantageous.
All of these practically relevant criteria are evaluated to determine which node to move to based on the current and last node. The importance of each criterion is set by the user based on the requirements of his or her application. An overview of the algorithm is given in Algorithms 2 and 3.

Algorithm 2 Subcircle Function.

```
FIND SUBCIRCLE
while starting node is not reached do
  if feasible nodes exist then
    calculate metrics for potential next nodes
    rank nodes according to user criteria
    add node to K_Sub
  else
    return K_Sub
  end if
end while
return K_Sub
```

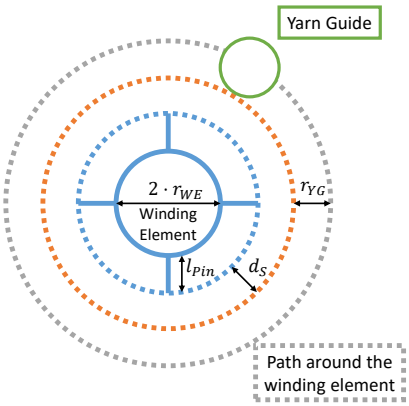

Figure 4: Schematic of the path of the yarn guide around the winding elements.

Algorithm 3 Graph-based Algorithm.

while node with open connections exists **do**
  find node with open connections
  while node is in stored K_{Sub} **do**
    if all nodes checked **then**
      genetic optimization of non-blocking connections
      insert optimized sequence in K
      update adjacency matrices **continue**
    end if
  end while
  find subcircle K_{Sub}
  if $K_{Sub}[1] \neq K_{Sub}[end]$ **then**
    store K_{Sub}
    continue
  end if
  if K_{Sub} does not block and is not blocked **then**
    insert K_{Sub} in overall circle K
  else
    find fastest path $K_{connect}$ between last node of K and first node of K_{Sub} via Dijkstra's algorithm
    insert $K_{connect}$ and K_{Sub} at the end of K
  end if
  update adjacency matrices
end while
return K

The resulting sequence of nodes K then serves as the input for the spatial path planning described in the following section.

3 Path planning in three-dimensional space

To successfully convert the node sequence to a sequence of motions for the robot end-effector several steps have to be taken. In our approach we first plan the motions on the x-y-plane with the limitation that the tubes and their winding elements are oriented in or only at small angles ($< 5°$) to the z-axis. Usually, the winding elements' projections onto the x-y-plane are round but arbitrary shapes can be coped with by discretization of their convex hull. For clarity, only circular elements are considered in the following description.
The first thing to consider is the distance between yarn guide and winding elements to ensure collision-free motions. Therefore, the yarn guide is programmed to move around the winding elements on a circle. The radius of this circle is the sum of the winding element's radius r_{WE}, its pin length l_{Pin}, the yarn guide's radius r_{YG}, and a safety distance d_S, as illustrated in Fig 4.

During the path planning the yarn guide is always routed around the winding elements on this perimeter to guarantee zero collisions between the yarn guide and the winding elements. Therefore, the path between winding elements is always checked for intersections with the perimeters of the elements to be connected as well as every other winding element. However, not only the path around the winding elements is essential but also the direction, in which the yarn guide moves around them. This is illustrated in **Figure 5**. If the next element (no. 3) is on the left of the two previous ones, the path around the current winding element (no. 2) needs to be conducted counterclockwise. Equivalently, if it is positioned on the right, the path needs to be conducted clockwise. Otherwise, either the winding element will not be incorporated in the structure or an unnecessary length of yarn will be deposited on the winding element. In case, the current element (no. 4) is on a straight line between the previous and next elements, the direction has to be identical to the one on the previous pin. These rules are implemented in Matlab to form the basis of our spatial path planning algorithm. This abstraction and planning step is purely done in 2D, i.e. the x-y-plane.

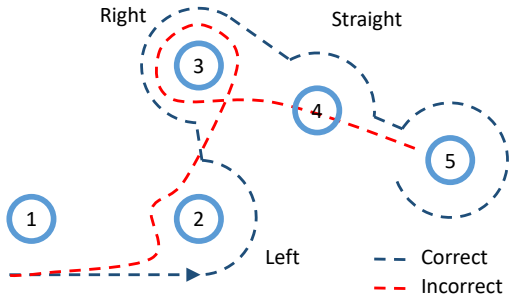

Figure 5: Path of the yarn guide between winding elements and the correct and incorrect traveling directions.

3.1 Deposition of yarn on the winding elements

However, to successfully deposit yarns on the winding elements not only the path around and in between the winding elements is important but also the lay-in mechanism where the yarn is positioned between the pins. Therefore, a part of the path around the winding elements is identified as the lay-in section. During the lay-in section, the yarn guide needs to be at the correct height at the right position on the x-y-plane in order to successfully deposit the yarn. This is illustrated by the top-view schematic in **Figure 6**.

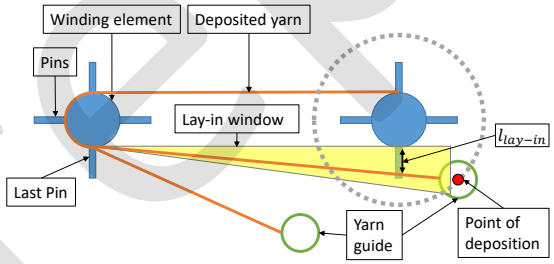

Figure 6: Schematic of the path of lay-in process as a top-view.

To determine the section of the perimeter that is critical for the lay-in process the base of the last pin is used. From this point, lines are drawn with the secondary points being located at the end of the next pin but shifted out and in (labeled l_{lay-in}) according to the yarn diameter plus a safety margin. We used double the yarn diameter, which worked well in the tested cases. Now the intersections of these lines with the perimeter define the lay-in section. Once the second of these points is reached (labeled "Point of deposition"), the yarn has been deposited successfully between the pins. During the lay-in section, the height of the yarn guide is critical as the side-view schematic in **Figure 7** shows.

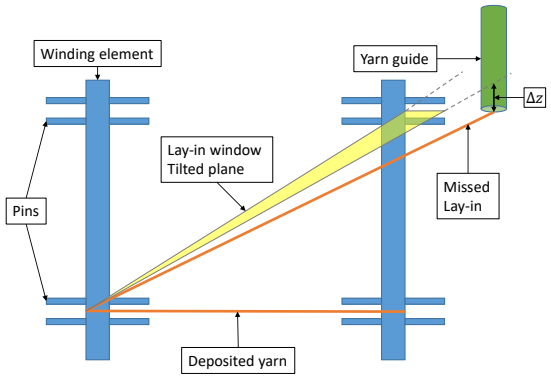

Figure 7: Schematic of the path of lay-in process as a side-view.

In particular, if the nodes are not at the same height. Due to the safety distance between the yarn guide and winding elements, the yarn to be deposited is not at the same height as the pins. This difference Δz leads to missed lay-in processes. Therefore, the z-coordinate of the path during the lay-in section will be chosen based on a tilted plane constructed from three points: the base points of the last and current pin on the winding elements and the tip of the pins of the current winding element. When the tip of the yarn guide travels on that plane, the yarn will be at the correct height during the lay-in procedure.

3.2 Transition around and in between the winding element

To determine the z-coordinate of the path around and in between winding elements that are not part of the lay-in section the same plane is used but superimposed by the positions of already deposited yarns that need to be avoided. This height map is generated by Matlab's "scatteredInterpolant" function and outputs the z-coordinates to the x- and y-values calculated in the previous steps.

4 Path planning and winding of a demonstrator structure

Initially, both the graph-based algorithm and the spatial path planning were tested on two-dimensional structures with increasing complexity. Starting from the simplest possible structure of two connected nodes, going over to four connected nodes with a cross and six unevenly spaced nodes. The basic configurations are displayed in **Figure 8** along with the winding path visualized in Matlab. These are similar to the structures shown by Oval et al..[27] These are evaluated for different distances between nodes and layers of reinforcement yarn. Due to the limited reach of the available KUKA KR6 robot, the calculated winding is validated by winding polyester yarns around 3D-printed winding element.

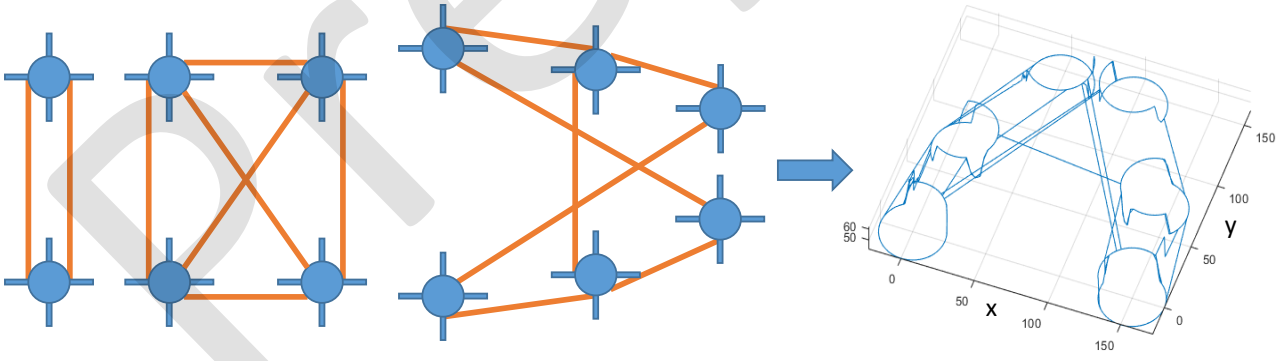

Figure 8: Schematics and winding path for the two-dimensional demonstrator structures.

After successfully winding these three structures a three-dimensional case was chosen to demonstrate

that the approach also works for more complex winding geometries than those demonstrated in literature before. The structure is based on a topology optimized truss with four fixed points and four points where loads in different directions are applied, so the structure in total is torsionally distorted. With regard to this loading scenario the topology optimization leads to a truss structure with crossing reinforcement yarns between the winding elements as illustrated in **Figure 9**.

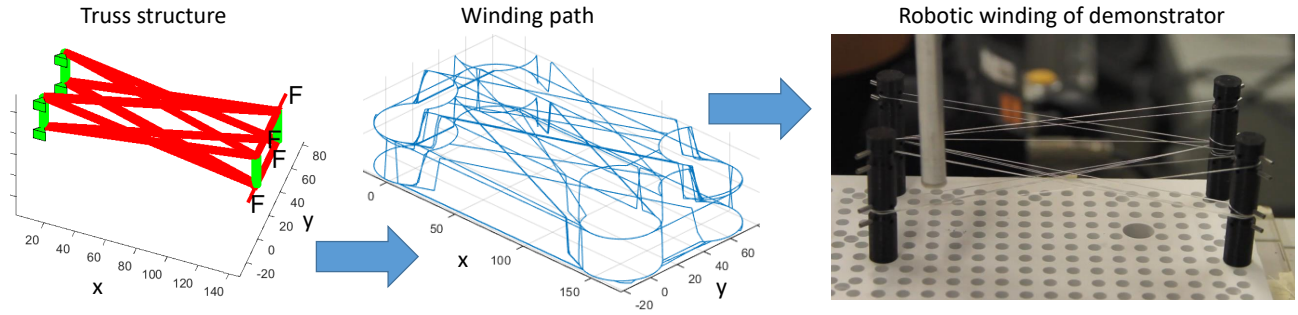

Figure 9: Design, path planning, and real-world winding of the three-dimensional demonstrator structure.

From these, the winding path is derived as shown and finally, the winding process is demonstrated on lab-scale. Videos of the winding process are available as supplementary material.

5 Conclusion

In summary, we have designed and validated a two-step algorithm to automatically plan the trajectories for coreless robotic winding. The approach allows for arbitrary numbers of yarns to be used and nodes on different heights even if they are positioned one above the other. After implementing the algorithms in Matlab, they were validated on four different structures. However, this needs to be extended to more geometries in the future. Other avenues of research to pursue are:

- In our set-up the angle of the end-effector is kept constant. At times this leads to small bending radii of the fiber around the edge of the yarn guide, which is particularly disadvantageous for brittle yarns such as carbon fibers. An improvement might be achieved by inclining the yarn guide at an angle closer to the fiber trajectory.
- Not all truss structures can be manufactured with this type of coreless robotic winding. There may be combinations of three or more trusses, which cover each other, making them impossible to deposit. Possible improvements in that regard are either to develop new approaches to topology optimization or introduce more degrees of freedom in the process. The second option includes the use of more than one manipulator or additional actuators on the end-effector to guide yarns around already deposited ones. But because this drives cost and complexity, the development of novel topology optimization strategies is also promising. If the process constraints could already be coped with during the optimization step, resulting in a truss structure that is definitely processable, the presented approach could quickly and automatically yield tailored high-performance composites.
- Further improvements can be made with regard to the winding elements, the end-effector, and the impregnation process of the reinforcement yarns. Both are critical for a strong composite structure and reliable winding process but have only received marginal research efforts from the scientific community.
- Finally, the presented algorithm is designed to avoid collisions between the yarn guide, winding elements, and reinforcement yarns. Still, it is currently not possible to test the output digitally. Therefore, a simulation environment could be beneficial to test and adjust the path before employing it on the actual system.

In conclusion, the described algorithm presents a major step forward to automatic path planning of the winding process for topology optimized truss structures. However, many challenges remain. Therefore, the coreless robotic winding technology is a field with continuing relevance and many research opportunities to be approached.

6 Experimental Section

6.1 Coreless filament winding setup

To test the developed 3D winding procedure a KUKA KR 6 robot was used (KUKA AG, Augsburg, Germany) with an aluminum tube as the end-effector. The tool center point was taught using KUKA's teaching procedure. A thin polyester thread was used for the minituarized set-up and wound around 3D-printed (Fused Filament Deposition) winding elements with 2 mm thick aluminum pins. The yarn was tensioned by a yarn guide with a 100 g weight, which were positioned over the robot together with the let-off spool. Corresponding geometry files are available from the authors upon request.

6.2 Conversion to a robot program for a 6-axis system

After the three-dimensional coordinates have been calculated for the node sequence of K, an additional Matlab script converted the coordinates to the KUKA Robot Language (KRL). Based on templates according to the individual robot, which in our case is a KUKA KR6 with a reach of 910 mm, the sequence and points are written to the .dat- and .src-files. If the winding of one structure exceeds the limited number of points within one program, they are divided into subprograms, which are called from a main program. The motions of the robot can be programmed to be either linear (SLIN, slow but accurate) or point-to-point (SPTP, faster but less accurate). For our cases, the SPTP-option was sufficiently accurate and used in the winding of the exemplary structure described in section 4. We wrote the algorithms in Matlab due to its ease-of-use for debugging and integrated functions to quickly develop such algorithms. However, this is hardly suitable for real-world production environments and should be addressed in the future.

Supporting Information
As the supplementary materials two videos of the winding process can be found using the following DOI: 10.5281/zenodo.8279498 . The first video displays a part of the winding process of the three-dimensional configuration. The second part shows a section of the winding of the six-node configuration, where a yarn is wound around one of the winding elements.

Acknowledgements
The authors are grateful for the funding by the Deutsche Forschungsgemeinschaft (DFG, German Research Foundation) – SFB/TRR280, Project-ID 417002380.

References

[1] M. Crippa, G. Oreggioni, D. Guizzardi, M. Muntean, E. Schaaf, E. Lo Vullo, E. Solazzo, F. Monforti-Ferrario, J. Olivier, E. Vignati, *Fossil CO2 and GHG emissions of all world countries: 2019 report*, volume 29849 of *EUR*, Publications Office of the European Union, Luxembourg, **2019**.

[2] A. Ilki, D. Çavunt, Y. S. Çavunt, editors, *Building for the Future: Durable, Sustainable, Resilient*, Lecture Notes in Civil Engineering. Springer Nature Switzerland, Cham, **2023**.

[3] B. Beckmann, J. Bielak, S. Bosbach, S. Scheerer, C. Schmidt, J. Hegger, M. Curbach, *Civil Engineering Design* **2021**, *3*, 3 99.

[4] M. von Zuben, C. Cherif, In AUTEX2019, editor, *19th World Textile Conference on Textiles at the Crossroads*, volume 19. **2019** .

[5] N. Minsch, M. Müller, T. Gereke, A. Nocke, C. Cherif, *Journal of Composite Materials* **2019**, *53*, 15 2077.

[6] S. Bodea, P. Mindermann, G. T. Gresser, A. Menges, *3D printing and additive manufacturing* **2022**, *9*, 3 145.

[7] I. Koustas, T. Papingiotis, G.-C. Vosniakos, A. Dine, *Procedia Manufacturing* **2018**, *17* 919.

[8] J. Mlýnek, M. Petrů, T. Martinec, S. S. R. Koloor, *Polymers* **2020**, *12*, 5.

[9] L. Sorrentino, E. Anamateros, C. Bellini, L. Carrino, G. Corcione, A. Leone, G. Paris, *Composite Structures* **2019**, *220* 699.

[10] R. La Magna, F. Waimer, J. Knippers, *Construction and Building Materials* **2016**, *127* 1009.

[11] P. Mindermann, M.-U. Witt, G. T. Gresser, *Composites Part A: Applied Science and Manufacturing* **2022**, *154* 106763.

[12] A. Paolini, S. Kollmannsberger, E. Rank, *Additive Manufacturing* **2019**, *30* 100894.

[13] F. Safari, A. Kami, V. Abedini, *Polymers and Polymer Composites* **2022**, *30* 096739112210987.

[14] D. Yavas, Z. Zhang, Q. Liu, D. Wu, *Composites Part B: Engineering* **2021**, *204* 108460.

[15] C. J. Hunt, F. Morabito, C. Grace, Y. Zhao, B. K. Woods, *Composite Structures* **2022**, *284* 115120.

[16] S. Bodea, C. Zechmeister, N. Dambrosio, M. Dörstelmann, A. Menges, *Automation in Construction* **2021**, *126* 103649.

[17] R. Oval, E. Costa, M. Nuh, D. Thomas-McEwen, J. Orr, P. Shepherd, In *Proceedings of IASS Annual Symposia*, volume 2020. **2020** 1–11.

[18] S. Gantner, P. Rennen, T. Rothe, C. Hühne, N. Hack, In R. Buswell, A. Blanco, S. Cavalaro, P. Kinnell, editors, *Third RILEM International Conference on Concrete and Digital Fabrication*, volume 37 of *RILEM Bookseries*, 391–396. Springer International Publishing, Cham, ISBN 978-3-031-06115-8, **2022**.

[19] Y. Ou, D.-W. Bao, G.-Q. Zhu, D. Luo, *3D printing and additive manufacturing* **2022**, *9*, 2 109.

[20] N. Minsch, F. H. Herrmann, T. Gereke, A. Nocke, C. Cherif, *Procedia CIRP* **2017**, *66* 125.

[21] N. Minsch, M. Müller, T. Gereke, A. Nocke, C. Cherif, *Journal of Composite Materials* **2018**, *52*, 22 3001.

[22] L. Sorrentino, M. Marchetti, C. Bellini, A. Delfini, F. Del Sette, *Composite Structures* **2017**, *164* 43.

[23] B. Beckmann, V. Adam, S. Marx, R. Chudoba, J. Hegger, M. Curbach, In A. Ilki, D. Çavunt, Y. S. Çavunt, editors, *Building for the Future: Durable, Sustainable, Resilient*, volume 350 of *Lecture Notes in Civil Engineering*, 1242–1251. Springer Nature Switzerland, Cham, ISBN 978-3-031-32510-6, **2023**.

[24] J. Wunnenberg, A. Rjosk, C. Neinhuis, T. Lautenschläger, *Biomimetics (Basel, Switzerland)* **2021**, *6*, 2.

[25] D. Friese, L. Hahn, C. Cherif, *Materials Science Forum* **2022**, *1063* 101.

[26] Z. Hu, O. Vambol, In M. Nechyporuk, V. Pavlikov, D. Kritskiy, editors, *Integrated Computer Technologies in Mechanical Engineering - 2021*, volume 367 of *Lecture Notes in Networks and Systems*, 863–873. Springer International Publishing, Cham, ISBN 978-3-030-94258-8, **2022**.

Table of Contents

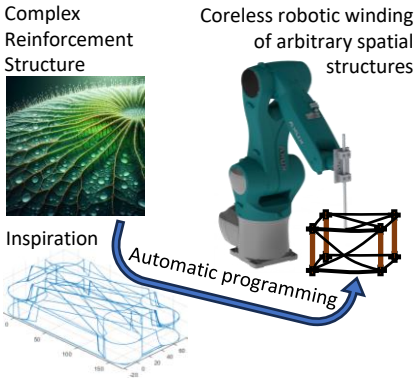

This article presents a novel two-step approach for automating the 3D coreless winding of high performance composites for lightweight or civil engineering applications. Inspiration for such highly load-adapted structures can be drawn from nature or topology optimization. With the presented approach unnecessary surplus material is minimized and the ultra high strength of carbon or basalt fibers is maximally exploited.

[27] R. Oval, E. Costa, D. Thomas-McEwen, S. Spadea, J. Orr, P. Shepherd, In *ISARC 2020: The 37th International Symposium on Automation and Robotics in Construction*. **2020** 1541–1548.

[28] G. Dreifus, K. Goodrick, S. Giles, M. Patel, R. M. Foster, C. Williams, J. Lindahl, B. Post, A. Roschli, L. Love, V. Kunc, *3D printing and additive manufacturing* **2017**, *4*, 2 98.

[29] H. A. Eiselt, M. Gendreau, G. Laporte, *Operations Research* **1995**, *43*, 3 399.

[30] H. Wang, Y. Yu, Q. Yuan, In *2011 second international conference on mechanic automation and control engineering*. IEEE, **2011** 1067–1069.